Ab Initio and Density Functional Theory Calculations on Heteroatom Analogues of Trimethylenemethane Radical Ions. Can a Quartet Be the Ground State?

Eric C. Brown and Weston Thatcher Borden*,†

Contribution from the Department of Chemistry, Box 351700, University of Washington, Seattle, Washington 98195-1700

Received: October 19, 2001; In Final Form: January 18, 2002

To answer the question, "Can a quartet be the ground state of heteroatom analogues of trimethylenemethane (TMM)?", B3LYP, CASSCF, and CASPT2 calculations have been performed on the lowest doublet and quartet states of the positive and negative radical ions of TMM and of several heteroatom-substituted analogues. Of the molecules on which calculations were performed, all those containing three π electrons, including $AlO_3^{\bullet}$, were found to have doublet ground states. However, a quartet ground state was computed for $O(SiH_2)_3^{\bullet+}$, a radical ion containing five π electrons. Calculations on $H_3^{\bullet}$ and $HeH_3^{\bullet}$ models revealed a similar difference between the three- and five-electron cases. A doublet was computed to be the ground state of $H_3^{\bullet}$ at all D_{3h} geometries, but at some He−H distances the quartet was computed to be the ground state of D_{3h} $HeH_3^{\bullet}$. The model calculations lead to an explanation of why radicals containing three π electrons are all predicted to have doublet ground states; whereas, the quartet is computed to be the ground state of at least one radical containing five π electrons.

Since its conception by Moffitt[1] in 1948 and its synthesis and spectroscopic observation by Dowd[2] in 1966, trimethylenemethane (TMM) and its derivatives have become the most thoroughly studied non-Kekulé hydrocarbon diradicals.[3] The ground state of TMM has long been known to be a triplet,[2,4] as expected from both qualitative molecular orbital (MO)[5] and valence-bond (VB)[6] theories. The size of the singlet−triplet energy splitting has been measured[7] and found to be in good agreement with the results of high-level ab initio calculations.[8]

TMM
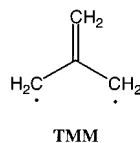
Much less is known about the radical ions of TMM than about the neutral diradical. The parent radical cation (TMM$^{\bullet+}$) has been generated by Shiotani and co-workers and studied by EPR.[9] As predicted computationally, 10 years before the EPR study was performed,[10] the doublet ground state was found to pseudorotate from one Jahn−Teller-distorted geometry to another with little or no barrier. Derivatives of TMM$^{\bullet+}$ have been formed as reactive intermediates by one-electron oxidation of methylenecyclopropanes.[11]

Even less is known about the TMM radical anion (TMM$^{\bullet-}$) than about the radical cation. TMM$^{\bullet-}$ was generated in the gas-phase by Hu and Squires and used to obtain the negative ion photoelectron spectrum of TMM.[7] In the same study, the results of CASSCF and UB3LYP calculations on the two, Jahn−Teller distorted, C_{2v} states of TMM$^{\bullet-}$ were reported. The $^2A_2$ state was computed to be 0.1−0.6 kcal/mol lower in energy than the $^2B_1$ state.[7]

Recently, Iwamura and co-workers have prepared derivatives of TMM radical ions in which the three methylene groups were

replaced by *p*-(*tert*-butylnitroxyl)phenyl groups and the central carbon was replaced by boron or by nitrogen.[12] $B(CH_2)_3^{\bullet}$ is isoelectronic with TMM$^{\bullet+}$, and $N(CH_2)_3^{\bullet}$ is isoelectronic with TMM$^{\bullet-}$.

EPR magnetic susceptibility studies showed that the $B(CH_2)_3^{\bullet}$ and $N(CH_2)_3^{\bullet}$ derivatives prepared by Iwamura and co-workers had doublet ground states. However, the presence of a thermally populated, excited quartet state was detected in both compounds. UB3LYP calculations on a model for the aza compound, in which the *tert*-butyl substituents on the nitroxyl groups were replaced by methyls, gave a doublet-quartet energy separation that was in good agreement with that measured.[12]

Iwamura's study raises the question of whether it might be possible to prepare heteroatom analogues of TMM radical ions in which the ground state is a quartet, rather than a doublet. In this paper we address this question and report the results of ab initio and density functional theory (DFT) calculations on the doublet-quartet energy differences (ΔE_{DQ}) in planar $X(CH_2)_3$ radicals with three π electrons (X = Al, B, and C^+) and five π electrons (X = C^-, N, and O^+). We also describe how replacement of the three methylene groups in $Al(CH_2)_3^{\bullet}$ by oxygen atoms and in $O(CH_2)_3^{\bullet+}$ by SiH_2 groups affects the calculated values of ΔE_{DQ}.

We have found that our computational results on molecules containing three and five π electrons are mirrored by the results of calculations on $H_3^{\bullet}$ and $HeH_3^{\bullet}$ models. These models provide an explanation for why the quartet can fall below the doublet in properly designed heteroatom derivatives of TMM$^{\bullet-}$ but not in heteroatom derivatives of TMM$^{\bullet+}$.

Computational Methodology

We were interested in comparing the relative energies of the doublet and quartet states of the $X(CH_2)_3$ radicals with fully conjugated π systems, since at such geometries the quartet has the best chance of being competitive in energy with the lowest

† Email address: borden@chem.washington.edu.

doublet state. Therefore, most of our calculations were performed on molecules that were constrained to be planar. The geometries of the doublet and quartet states of molecules, thus constrained, were optimized in the C_{2v} and D_{3h} point groups, respectively.

Especially for the $X(CH_2)_3$ radicals containing five π electrons, pyramidalization of X and/or the peripheral CH_2 groups was computed to be energetically favorable. Consequently, for such molecules, the optimized C_{2v} and D_{3h} geometries are not energy minima but are, instead, stationary points of higher order, usually with several imaginary vibrational frequencies. Therefore, the relative energies of the doublet and quartet states of such molecules were not corrected for differences between their zero-point vibrational energies.

Unless otherwise specified, all calculations were performed with the 6-31+G(d) basis set.[13] Unrestricted (U)DFT calculations were carried out utilizing Becke's three-parameter, hybrid functional[14] and the nonlocal correlation functional of Lee, Yang, and Parr[15] (B3LYP). The *Gaussian 98* suite of programs[16] was used to perform the UB3LYP calculations.

CASSCF calculations were carried out with the *GAMESS* package of ab initio programs.[17] The active space for the CASSCF calculations consisted of the number of π electrons in each species [e.g. three for $B(CH_2)_3^\bullet$ and five $N(CH_2)_3^\bullet$], distributed among the four π MOs of TMM. To include the effects of dynamic electron correlation[18] in the (3/4)CASSCF and (5/4)CASSCF calculations, CASPT2[19] single point calculations were performed at the CASSCF optimized geometries, using the *MOLCAS* suite of programs.[20] Absolute UB3LYP, CASSCF, and CASPT2 electronic energies and the optimized UB3LYP and CASSCF geometries for each of the low-lying electronic states of all the molecules discussed in this paper are available as Supporting Information.

Results and Discussion

Corrections for Artifactual Symmetry Breaking. In the lowest doublet state of a planar $X(CH_2)_3$ radical that contains either three or five π electrons, an odd number of electrons must be placed in the pair of nonbonding π MOs. At D_{3h} geometries these MOs belong to the degenerate e'' representation of the D_{3h} point group. Since the e_x'' and e_y'' NBMOs are degenerate at D_{3h} geometries, at such geometries the energies of the $^2E_x''$ and $^2E_y''$ states that result from singly occupying one or the other of these two NBMOs should be exactly the same.

However, in practice, the computed energies of the two states that result from singly occupying one or the other of the two NBMOs usually do not have exactly the same energy. As discussed in detail elsewhere,[10,21] approximate wave functions usually show artifactual symmetry breaking, because at D_{3h} geometries the two lowest doublet wave functions for $X(CH_2)_3$ radicals do not really have pure E_x'' and E_y'' symmetry. Instead the wave functions belong to, respectively the A_2 and B_1 representations of the C_{2v} subgroup of D_{3h}. Since A_2 and B_1 are not degenerate representations (the C_{2v} point group has none), at D_{3h} geometries the two lowest doublet wave functions generally do not have the same energy.

Like the pure $^2E_x''$ and $^2E_y''$ wave functions to which they correspond, the $^2A_2$ and $^2B_1$ states each undergo a first-order Jahn−Teller distortion[22] to a C_{2v} geometry of lower symmetry. One of these states is expected to represent the maxima and the other the minima along the lowest energy pathway for pseudorotation of the lowest doublet state of an $X(CH_2)_3$ radical around a D_{3h} geometry.[21] However, if the energies of these two states are spuriously computed to be different at D_{3h} geometries,

TABLE 1: Relative Energies (kcal/mol), Calculated for the Electronic States in XY₃ Radicals Containing Three π Electrons

molecule	method	$E(^2B_1) -$ $E(^2A_2)^a$	$E(^2B_1)^{corr} -$ $E(^2A_2)^b$	$E(^4A_1'') -$ $E(^2A_2)^c$
$C(CH_2)_3^{\bullet+}$	CASSCF	0.3	0.2	56.1
	CASPT2	0.1	−0.2	62.7
	B3LYP	2.0	−0.3	63.0
$B(CH_2)_3$	CASSCF	0.0	0.0	17.2
	CASPT2	0.0	−0.1	23.3
	B3LYP	6.9	−2.3	23.7
$Al(CH_2)_3$	CASSCF	0.1	−0.2	2.7
	CASPT2	0.0	0.0	4.4
	B3LYP	18.7	0.4	4.5
AlO_3	CASSCF	0.0	0.0	0.4
	CASPT2	0.0	0.0	1.0
	B3LYP	48.5	−1.8	0.9

^{a} Energy, which, when subtracted from that of $^2B_1$, would make the energy of $^2B_1$ the same as that of $^2A_2$ at the D_{3h} equilibrium geometry of $^4A_1''$. ^{b} Relative energies of $^2B_1$ and $^2A_2$ at their equilibrium geometries, after correction of the energy of $^2B_1$ for the effect of artifactual symmetry breaking at the D_{3h} geometry of $^4A_1''$. ^{c} ΔE_{DQ}.

TABLE 2: Relative Energies (kcal/mol), Calculated for the Electronic States in XY₃ Radicals Containing Five π Electrons

molecule	method	$E(^2B_1) -$ $E(^2A_2)^a$	$E(^2B_1)^{corr} -$ $E(^2A_2)^b$	$E(^4A_1'') -$ $E(^2A_2)^c$
$C(CH_2)_3^{\bullet-}$	CASSCF	1.2	−1.1	49.2
	CASPT2	−0.9	0.6	42.9
	B3LYP	0.2	0.2	40.5
$N(CH_2)_3$	CASSCF	−0.2	−0.6	32.5
	CASPT2	0.1	0.3	38.0
	B3LYP	2.3	−0.7	38.0
$O(CH_2)_3^{\bullet+}$	CASSCF	0.0	−0.1	5.1
	CASPT2	0.0	−0.1	8.9
	B3LYP	17.7	−4.1	8.0
$O(SiH_2)_3^{\bullet+}$	CASSCF	0.0	0.0	−0.9
	CASPT2	0.0	0.0	−0.8
	B3LYP	22.1	0.0	−0.1

^{a} Energy, which, when subtracted from that of $^2B_1$, would make the energy of $^2B_1$ the same as that of $^2A_2$ at the D_{3h} equilibrium geometry of $^4A_1''$. ^{b} Relative energies of $^2B_1$ and $^2A_2$ at their equilibrium geometries, after correction of the energy of $^2B_1$ for the effect of artifactual symmetry breaking at the D_{3h} geometry of $^4A_1''$. ^{c} ΔE_{DQ}.

there is every reason to believe that this energetic advantage of one state over another will also be manifested in the relative energies of the states at the optimized C_{2v} geometry of each.

The simplest way to correct for this effect of artifactual symmetry breaking, due to the approximate nature of the electronic wave functions, is to subtract the energy difference between $^2A_2$ and $^2B_1$ at a D_{3h} geometry (e.g., at the optimized geometry of the quartet, $^4A_1''$) from the energy difference between these two doublet states at the optimized C_{2v} geometry of each. For example, our calculations almost invariably found that, at the D_{3h} geometry of $^4A_1''$, $^2B_1$ was higher in energy than $^2A_2$. The energy that has to be subtracted from the energy of $^2B_1$, to make it degenerate with $^2A_2$ at the optimized D_{3h} geometry of $^4A_1''$ is shown in the first column of Tables 1 and 2. The second column shows the energy of $^2B_1$, relative to $^2A_2$, at the optimized C_{2v} geometry of each state, after this correction for artifactual symmetry breaking has been applied.

The results in Tables 1 and 2 show that artifactual symmetry breaking in $^2A_2$ and $^2B_1$ has a much larger effect on the relative UB3LYP energies of these two states than on their relative CASSCF or CASPT2 energies. The effect of artifactual symmetry breaking on the UB3LYP relative energies increases with
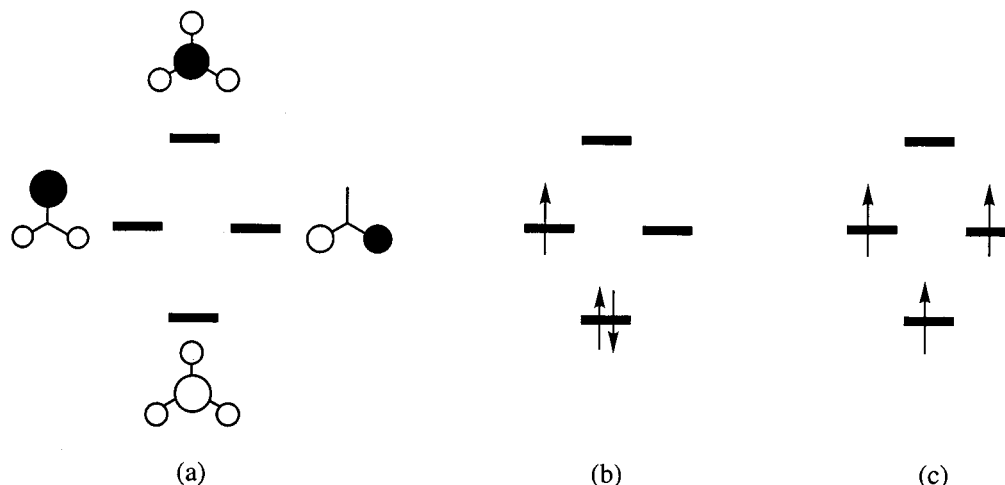
Figure 1. Schematic depiction of (a) the π MOs for TMM and how they are occupied in the (b) $^2E_y''$ and (c) $^4A_1''$ states of an XY$_3$ radical containing three π electrons. Only the top lobe of each 2p AO is shown.

the difference between the electronegativities of the central and terminal atoms.

As the difference between the electronegativities of the central and terminal atoms in XY$_3$ increases, configurations, other than the one of lowest energy, become increasingly important for both doublet states (vide infra). Since the UB3LYP calculations are based on wave functions that consist of a single configuration, it is not at all surprising that, as the difference between the electronegativities of the central and terminal atoms in XY$_3$ increases, UB3LYP does a poorer job than CASSCF or CASPT2 of computing the relative energies of the two lowest doublet states.

Apparently, $^2B_1$, in which the unpaired electron occupies an orbital of the same symmetry (b$_1$) as the doubly occupied π orbital(s), is less well-described by a single configuration at the UB3LYP level than is $^2A_2$, in which the unpaired electron occupies an orbital of different symmetry (a$_2$) than the doubly occupied π orbital(s). The poorer quality of the UB3LYP wave functions for $^2B_1$, compared to those for $^2A_2$, is reflected, not only in the higher UB3LYP energies of $^2B_1$, relative to $^2A_2$, but also in the larger deviations of the values of $\langle S^2 \rangle$ for $^2B_1$ from the value of $\langle S^2 \rangle = {}^3/_4$ for a pure doublet wave function. Therefore, in discussing the UB3LYP results in Tables 1 and 2, we will use the $^2A_2$, rather than the $^2B_1$ energies.

As the quality of the wave functions for the components of a degenerate state improves, the amount of artifactual symmetry breaking decreases; and the energies of the components become more nearly the same at the geometry of highest symmetry. This can be clearly seen by comparing the sizes of the CASSCF and CASPT2 corrections for artifactual symmetry breaking in Tables 1 and 2 with the UB3LYP corrections. Except in C(CH$_2$)$_3$$^{\bullet-}$, the largest CASSCF correction is 0.3 kcal/mol, and the largest CASPT2 correction is 0.1 kcal/mol.

Effect of Including Dynamic Electron Correlation. Our (3/4)- and (5/4)CASSCF calculations do not include the effects of dynamic electron correlation between the σ and the π electrons,[18] but our CASPT2 calculations do. Therefore, there is every reason to expect the CASPT2 results for $E(^4A_1'') - E(^2A_2) = \Delta E_{DQ}$ in Tables 1 and 2 to be more accurate than the CASSCF results.

UB3LYP does not explicitly include any correlation between the σ and the π electrons in the Kohn−Sham orbitals from which the densities are computed. However, the effects of both dynamic and nondynamic electron correlation are included in the B3LYP functional, from which the energy is calculated.

Thus, perhaps it is not surprising that inspection of Tables 1 and 2 shows the energy differences between $^4A_1''$ and $^2A_2$, obtained by the CASPT2 and UB3LYP calculations, are generally in much better agreement with each other than with the CASSCF results. Consequently the following discussions of ΔE_{DQ} for the molecules in Tables 1 and 2 is based on the CASPT2 and UB3LYP results for the energy differences between $^4A_1''$ and $^2A_2$ in Tables 1 and 2, rather than on the CASSCF results.

Effect of Heteroatom Substitution on ΔE_{DQ} in C(CH$_2$)$^{\bullet+}$. The values of ΔE_{DQ} in Table 1 for the X(CH$_2$)$_3$ radicals with three π electrons decrease in the order, X = C$^+$ > X = B > X = Al. The reasons for this decrease are easy to understand from the X(CH$_2$)$_3$ π MOs and how they are occupied in the lowest doublet and quartet states. The MOs and their occupancies in $^2A_2$ and $^4A_1''$ are depicted schematically in Figure 1.

The formation of $^4A_1''$ from either of the lowest doublet states requires the excitation of an electron from the bonding $1a_2''$ MO to the e$''$ NBMO that is empty. Therefore, the difference between the e$''$ and $1a_2''$ orbital energies plays a crucial role in determining the size of ΔE_{DQ} for the radicals in Table 1. Since $1a_2''$ is a bonding MO and e$''$ is nonbonding, ΔE_{DQ} should decrease with a decrease in the strength of the π bonds between the central atom, X, and CH$_2$. Thus, since π bond strengths decrease in the order π(C−C) > π(B−C) > π (Al−C),[23] the fact that ΔE_{DQ} decreases in the same order is easily understandable.

However, this is not the only manner in which the identity of X in X(CH$_2$)$_3$ affects the difference between the e$''$ and $1a_2''$ orbital energies and, hence, the size of ΔE_{DQ}. As shown in Figure 1, the e$''$ MOs have a node at the central atom, whereas $1a_2''$ does not. Consequently, a $1a_2'' \rightarrow$ e$''$ excitation transfers electron density from X to the peripheral carbons. Thus, the less electronegative X is, relative to C, the smaller the e$'' - 1a_2''$ orbital energy difference and the lower the calculated size of the ΔE_{DQ} energy difference in Table 1.

Replacing Y = CH$_2$ in XY$_3$ with a more electronegative group or atom should also decrease the size of the e$'' - 1a_2''$ orbital energy difference and, hence, the size of ΔE_{DQ}. As shown in Table 1, going from Al(CH$_2$)$_3$ to AlO$_3$ is computed to lower the CASPT2 value of ΔE_{DQ} from 4.4 kcal/mol to only 1.0 kcal/mol. Since an Al−O π bond is stronger than an Al−C π bond,[23] this decrease in ΔE_{DQ} is clearly not due to a decrease in π bond strengths but to the greater electronegativity of O, relative to CH$_2$.

TABLE 3: (3/3)CASSCF/6-311G(p) Energies (kcal/mol) and Coefficients of the Configurations in the Wave Function (Equation 13) for the $^2E'$ State of D_{3h} $H_3{}^\bullet$ as a Function of the Distance, R, from the Center of Mass (Energies Relative to the D_{3h} Minimum for $^2E'$ at $R = 0.65$ Å)

R (Å)	c_1	c_2	c_3	$E(^2E')$	$E(^4A_2')$	ΔE_{DQ}
0.65	0.975	0.134	0.181	0^a	158.24	158.24
1.0	0.859	0.286	0.427	12.47	52.74	40.27
1.5	0.683	0.471	0.559	20.06	24.26	4.2
2.0	0.608	0.546	0.576	20.86	21.18	0.32
2.5	0.585	0.569	0.577	20.91	20.91	0.0
3.0	0.579	0.575	0.577	20.92	20.92	0.0

$^a E = -1.532765$ hartrees.

A Simple Model for XY$_3$ Radicals with Three π Electrons and Y Much More Electronegative than X. In a hypothetical XY$_3$ radical that is isoelectronic with $C(CH_2)_3{}^{\bullet+}$, if Y were *infinitely* more electronegative than X, all three π electrons would be localized in p-π AOs on the electronegative Y atoms. If there really were no delocalization of electrons into the empty p-π AO on X, this would be equivalent to not having a p-π AO on the central atom or to not having a central atom at all. Therefore, H$_3{}^\bullet$ with equal separations between all three hydrogens should provide an adequate model for the π system of such an XY$_3$ radical at D_{3h} geometries.[24]

Correlation between the three electrons in the three 1s orbitals of H$_3{}^\bullet$ can be handled by (3/3)CASSCF calculations. The results of (3/3)CASSCF/6-311G(p) calculations on H$_3{}^\bullet$ at D_{3h} geometries are given in Table 3. The Table shows that, as the distance, R, between the three hydrogen atoms and their collective center of mass decreases, the energy of the $^4A_2'$ state rises monotonically, while that of the $^2E'$ state decreases by 20.9 kcal/mol between $R = 4.00$ Å and the D_{3h} minimum at $R = 0.65$ Å. Consequently, although the energies of $^4A_2'$ and $^2E'$ are essentially the same at $R = 4.0$ Å, the energy of $^4A_2'$ never falls below that of $^2E'$. Jahn–Teller distortions of $^2E'$ from D_{3h} geometries would, of course, further stabilize the doublet state.[24]

The results in Table 3 of the CASSCF calculations on the H$_3{}^\bullet$ model indicate that a doublet should also be the ground state of an XY$_3$ radical, containing three π electrons, even if Y were infinitely more electronegative than X. To understand why a doublet is expected to be the ground state, even under those circumstances most likely to provide the smallest values of ΔE_{DQ}, it is instructive to continue to exploit the simple H$_3{}^\bullet$ model.

Placing one electron in each 1s AO (ϕ) of H$_3{}^\bullet$ minimizes the Coulombic repulsion energy between electrons. For the $^4A_2'$ state this distribution of the three electrons is, of course, the only one allowed by the Pauli exclusion principle. Equation 1 gives the wave function for the component of the quartet in which the electron in each AO has spin α.

$$^4\Psi = |\phi_1^\alpha \phi_2^\alpha \phi_3^\alpha\rangle \tag{1}$$

However, the quartet is not the only state in which one electron can be localized in each 1s AO of H$_3{}^\bullet$. There is a $^2E'$ state in which this is also possible. The wave functions for its two components, $^2E_x'$ and $^2E_y'$ (respectively, $^2A_1$ and $^2B_1$ in C_{2v} symmetry), are given in eqs 2 and 3.

$$^2\Psi_x = \frac{1}{\sqrt{6}}[2|\phi_1^\beta \phi_2^\alpha \phi_3^\alpha\rangle - |\phi_1^\alpha \phi_2^\beta \phi_3^\alpha\rangle - |\phi_1^\alpha \phi_2^\alpha \phi_3^\beta\rangle] \tag{2}$$

$$^2\Psi_y = \frac{1}{\sqrt{2}}[|\phi_1^\alpha \phi_2^\beta \phi_3^\alpha\rangle - |\phi_1^\alpha \phi_2^\alpha \phi_3^\beta\rangle] \tag{3}$$

It is possible to rewrite the valence-bond wave functions in eqs 1–3 in terms of MOs. The normalized MOs, ψ, of D_{3h} H$_3{}^\bullet$ can be expressed as linear combinations of the 1s AOs. Equation 4 gives the wave function for the a_1 MO (ψ_1); and eqs 5 and 6 give, respectively, the wave functions for the degenerate pair of e_x (ψ_2) and e_y (ψ_3) MOs. The normalizations assume that the overlap between AOs is either negligible or is small enough to be neglected.

$$\psi_1 = \frac{1}{\sqrt{3}}(\phi_1 + \phi_2 + \phi_3) \tag{4}$$

$$\psi_2 = \frac{1}{\sqrt{2}}(\phi_2 - \phi_3) \tag{5}$$

$$\psi_3 = \frac{1}{\sqrt{6}}(2\phi_1 - \phi_2 - \phi_3) \tag{6}$$

Using eqs 4–6, each of the AOs can each be written as a linear combination of the MOs. Solving eqs 4–6 for each of the AOs affords

$$\phi_1 = \frac{\sqrt{3}}{3}\psi_1 + \frac{\sqrt{6}}{3}\psi_3 \tag{7}$$

$$\phi_2 = \frac{\sqrt{3}}{3}\psi_1 + \frac{\sqrt{2}}{2}\psi_2 - \frac{\sqrt{6}}{6}\psi_3 \tag{8}$$

$$\phi_3 = \frac{\sqrt{3}}{3}\psi_1 - \frac{\sqrt{2}}{2}\psi_2 - \frac{\sqrt{6}}{6}\psi_3 \tag{9}$$

Substituting eqs 7–9 into eq 1 gives the $^4A_2'$ wave function, expressed in terms of MOs. Not surprisingly, it reduces to the wave function in eq 10, which places one α electron in each MO.

$$^4\Psi = |\psi_1^\alpha \psi_2^\alpha \psi_3^\alpha\rangle \tag{10}$$

Using eqs 7–9, the $^2E'$ wave functions in eqs 2 and 3 can also be expressed in terms of the MOs in eqs 4–6. However, unlike the $^4A_2'$ wave function in eq 10, the $^2E'$ wave functions turn out to be linear combinations of configurations, each of which assigns the three electrons to a different set of MOs. The $^2E_x'$ wave function is given in eq 11, and the $^2E_y'$ wave function is given in eq 12.

$$^2\Psi_x = \frac{1}{\sqrt{3}}\left[|\psi_1{}^2\psi_2{}^\alpha\rangle - |\psi_1{}^\alpha\psi_3{}^2\rangle - \frac{1}{\sqrt{2}}(|\psi_1{}^\alpha\psi_2{}^\alpha\psi_3{}^\beta\rangle - |\psi_1{}^\alpha\psi_2{}^\beta\psi_3{}^\alpha\rangle)\right] \tag{11}$$

$$^2\Psi_y = \frac{1}{\sqrt{3}}\left[|\psi_1{}^2\psi_3{}^\alpha\rangle - |\psi_2{}^2\psi_3{}^\alpha\rangle - \frac{1}{\sqrt{2}}(|\psi_1{}^\alpha\psi_2{}^2\rangle - |\psi_1{}^\alpha\psi_2{}^3\rangle)\right] \tag{12}$$

At sufficiently large H–H distances, the quartet wave function in eq 10 has exactly the same energy as the degenerate doublet wave functions in eqs 11 and 12. However, as the hydrogen 1s AOs begin to overlap, two effects alter the relative energies of $^4A_2'$ and $^2E'$. One involves electron repulsion in the overlap regions between the hydrogen atoms, which selectively stabilizes the quartet. The other involves bonding between the hydrogens, which selectively stabilizes the doublet.
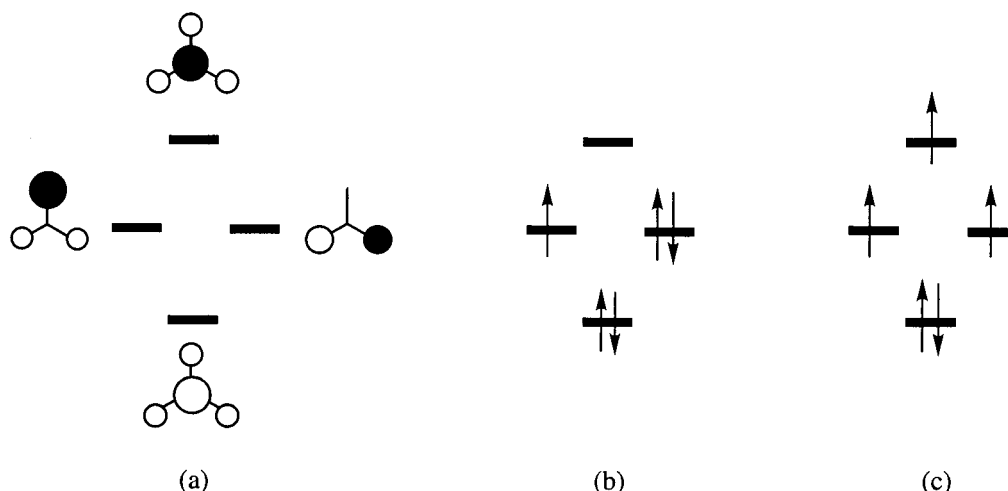
Heteroatom Analogues of TMM Radical Ions

J. Phys. Chem. A, Vol. 106, No. 12, 2002 **2967**

Figure 2. Schematic depiction of (a) the π MOs for TMM and how they are occupied in the (b) $^2E_y''$ and (c) $^4A_1''$ states of an XY$_3$ radical containing five π electrons. Only the top lobe of each 2p AO is shown.

The quartet wave function not only keeps the electrons from appearing in the same AO, but $^4\Psi$ also prevents the electrons from appearing simultaneously in the regions where two of the 1s AOs overlap. The doublet wave functions, $^2\Psi_x$ and $^2\Psi_y$, contain one electron that has opposite spin from the other two, and there is no prohibition against having a pair of electrons of opposite spin simultaneously in the same overlap region.[25] Consequently, the doublet wave functions each have a slightly higher Coulombic repulsion energy than the quartet, when the hydrogen 1s AOs begin to overlap.

On the other hand, in the quartet the interactions between the hydrogen atoms are all antibonding; but in the doublets some are bonding and some are antibonding. For example, using eq 2, it is easy to show that in $^2\Psi_x$ the interactions between ϕ_1 and both ϕ_2 and ϕ_3 are weakly bonding, but the interaction between ϕ_2 and ϕ_3 is antibonding. Similarly, using eq 3 it can be shown that just the reverse is true in $^2\Psi_y$; the interactions between ϕ_1 and both ϕ_2 and ϕ_3 are weakly antibonding, but the interaction between ϕ_2 and ϕ_3 is bonding. Overall, the doublet wave functions are each nonbonding. However, the quartet wave function is antibonding between all the hydrogens, and this confers an energetic advantage on the doublet.

Our CASSCF calculations find that, as the AOs of H$_3^\bullet$ begin to overlap, if the weights of the three types of configurations in each of the doublet wave functions in eqs 11 and 12 are kept equal, the quartet falls below the doublets in energy.[26] However, as the AOs begin to overlap, and ψ_1 is stabilized, relative to ψ_2 and ψ_3, the coefficients of the three types of configurations in eqs 11 and 12 do not remain equal. For example, in eq 13 for the $^2E_x'$ wave function, c_1, the coefficient of the configuration in which ψ_1 is doubly occupied, increases; and c_2, the coefficient of the configuration in which ψ_1 is empty decreases, as does the coefficient of the pair of configurations in which ψ_1 is singly occupied. The resulting increase in bonding between the hydrogens is what causes the doublets to be stabilized as the 1s AOs of the hydrogens begin to overlap.

$$^2\Psi_x = c_1|\psi_1{}^2\psi_2{}^\alpha\rangle - c_2|\psi_2{}^\alpha\psi_3{}^2\rangle - \frac{c_3}{\sqrt{2}}(|\psi_1{}^\alpha\psi_2{}^\alpha\psi_3{}^\beta\rangle - |\psi_1{}^\alpha\psi_2{}^\beta\psi_2{}^\alpha\rangle) \quad (13)$$

Table 3 gives the coefficients of the three configurations in the $^2\Psi_x$ wave function for H$_3^\bullet$ at several distances, R, between each of the hydrogens and their center of mass. The degeneracy of $^2E_x'$ and $^2E_y'$ at D_{3h} geometries ensures that, as the hydrogens

begin to overlap, the changes in the coefficients of the configurations in $^2\Psi_y$ are the same as those in the coefficients of the corresponding configurations in eq 13 for $^2\Psi_x$. Table 3 shows the changes in the coefficients of the configurations in the $^2E'$ wave functions are accompanied by a decrease in energy of this state by 20.9 kcal/mol on going from $R = 4.00$ Å to the D_{3h} geometry of minimum energy at $R = 0.65$ Å.

Bonding between the hydrogen 1s AOs favors the doublet state over the quartet in our H$_3^\bullet$ model for an XY$_3$ radical that contains three π electrons and in which Y is much more electronegative than X. Similarly, even if π bonding between X and Y does not provide any stabilization for the doublet state in such an XY$_3$ radical, bonding between the 2p-π AOs on Y will result in a doublet ground state. Consequently, we predict it is highly unlikely that an XY$_3$ radical, containing three π electrons, will ever be found in which the quartet is the ground state.

Effect of Heteroatom Substitution on ΔE_{DQ} in C(CH$_2$)$_3^{\bullet-}$. For X(CH$_2$)$_3$ molecules with five π electrons, ΔE_{DQ} in Table 2 shows exactly the opposite trend from ΔE_{DQ} in Table 1 for X(CH$_2$)$_3$ molecules with three π electrons. The value of ΔE_{DQ} in Table 2 decreases with increasing electronegativity of X in the order X = C$^-$ > X = N > X = O$^+$. Figure 2 shows that this decrease cannot be due to the fact that π bond strengths increase in the order π(C=C) < π(N=C) < π (O=C),[23] since formation of $^4A_1''$ from either of the lowest doublet states requires the excitation of an electron from the doubly occupied e'' NBMOs to the antibonding 2a$_2''$ MO. This excitation energy, and, hence, the size of ΔE_{DQ}, should increase with the strength of a π bond between X and CH$_2$; but the trend in Table 2 is just the opposite.

Instead, the decrease in ΔE_{DQ} with the electronegativity of X is due the fact that an e'' $\rightarrow$ 2a$_2''$ excitation transfers electron density from CH$_2$ to X. As already noted, e'' has a node at the central atom, X; whereas 2a$_2''$, like 1a$_2''$, does not. Therefore, the e'' $\rightarrow$ 2a$_2''$ excitation energy behaves exactly opposite to the 1a$_2''$ $\rightarrow$ e'' excitation energy and decreases with increasing electronegativity of X, relative to CH$_2$.

On going from X = C$^-$ to X = N in X(CH$_2$)$_3$, the decrease in ΔE_{DQ} is rather small. The decrease is calculated to be only 4.9 kcal/mol by CASPT2 and 1.8 kcal/mol by UB3LYP. We note, however, that the extra electron in $^2A_2$ C(CH$_2$)$_3^{\bullet-}$ is computed to be unbound (EA = -6.7 kcal/mol) by CASPT2 and barely bound (EA = 5.3 kcal/mol) by UB3LYP.[27] Since ΔE_{DQ} > 40 kcal/mol at both levels of theory, in the $^4A_1''$ state

TABLE 4: (3/3)CASSCF/6-311G(p) Energies (kcal/mol) and Coefficients of the Configurations in the Wave Function (eq 14) for the $^2E'$ state of D_{3h} HeH$_3^{\bullet}$ as a Function of the He−H Distance, R (Energies Relative to That of $^2E'$ at R = 4.0 Å

R (Å)	c_1	c_2	c_3	$E(^2E')$	$E(^4A_2')$	ΔE_{DQ}
1.0	0.355	0.794	0.489	148.55	158.83	−10.27
1.5	0.538	0.615	0.575	37.35	37.19	0.16^a
2.0	0.575	0.580	0.577	7.92	7.85	0.07
2.5	0.579	0.576	0.577	1.48	1.47	0.01
3.0	0.578	0.577	0.577	0.24	0.24	0.00
4.0	0.577	0.577	0.577	0^b	0.00	0.00

^{a} The maximum value of ΔE_{DQ} = 0.23 kcal/mol was found to occur around R = 1.6 Å. ^{b} E = −4.359325 hartrees.

of the radical anion the electron in the 2a$_2''$ MO is unbound, by ca. 50 kcal/mol at the CASPT2 level and by ca. 35 kcal/mol at UB3LYP.

Hence, in the $^4A_1''$ state of C(CH$_2$)$_3^{\bullet-}$ the electron in the 2a$_2''$ MO occupies a very diffuse, Rydberg-like, orbital, rather than a valence orbital, as in N(CH$_2$)$_3^{\bullet}$. Therefore, the difference between the values of ΔE_{DQ} in C(CH$_2$)$_3^{\bullet-}$ and N(CH$_2$)$_3^{.}$ does not really reflect the difference between the energies of the 2a$_2''$ valence orbitals in these two radicals.

In the $^4A_1''$ states of both N(CH$_2$)$_3^{\bullet}$ and O(CH$_2$)$_3^{\bullet+}$, 2a$_2''$ is a valence orbital. As a result, comparison of the ΔE_{DQ}, values in N(CH$_2$)$_3^{\bullet}$ and O(CH$_2$)$_3^{\bullet+}$ does reflect the effect of the difference between the electronegativities of N and O on the relative energies of the 2a$_2''$ MOs. It is for this reason that ΔE_{DQ} decreases by ca. 30 kcal/mol on going from N(CH$_2$)$_3^{\bullet}$ to O(CH$_2$)$_3^{\bullet+}$.

Replacing X by a more electronegative atom is one way to decrease the e$'' \rightarrow$ 2a$_2''$ excitation energy and, hence, the size of ΔE_{DQ}. Another way is to replace carbon in CH$_2$ by a more electropositive element, such as Si. The substitution of SiH$_2$ for CH$_2$ lowers the e$'' \rightarrow$ 2a$_2''$ excitation energy not only because Si is less electronegative than C, but also by virtue of the fact that a π bond to Si is weaker than a π bond to C.[23]

As shown in Table 2, the CASPT2 value of ΔE_{DQ} = 9.0 kcal/mol for O(CH$_2$)$_3^{\bullet+}$ decreases to −0.8 kcal/mol for O(SiH$_2$)$_3^{\bullet+}$. Thus, in planar O(SiH$_2$)$_3^{\bullet+}$ the quartet is actually predicted to fall slightly below the doublet in energy.[28]

A Simple Model for XY$_3$ Radicals with Five π Electrons and X Much More Electronegative than Y. Why is it possible to find a planar XY$_3$ radical with a quartet ground state when there are five π electrons, but not when there are three π electrons? As already discussed, an H$_3^{\bullet}$ model predicts that the doublet will always remain the ground state of XY$_3^{\bullet}$ when there are three π electrons, no matter how much more electronegative Y is than X. Therefore, it is reasonable to ask if a similarly simple model predicts that the quartet can become the ground state of XY$_3^{\bullet}$ when there are five π electrons and X is much more electronegative than Y.

In the model for the five-electron case we again used three hydrogen atoms, arranged in the geometry of an equilateral triangle, as Y in XY$_3^{\bullet}$. As a very electronegative central atom with two valence electrons we chose He. We then carried out (5/4)CASSCF/6-311G(p) calculations on HeH$_3^{\bullet}$ at D_{3h} geometries with different values of the He−H distance, R. The results are summarized in Table 4.

As shown in this Table, as R is decreased, the energies of both the $^2E'$ and $^4A_2'$ states of HeH$_3^{\bullet}$ increase monotonically. At small R $^2E'$ is the ground state. However, at intermediate values of R, the quartet falls below the doublet. Thus, at these values of R, the HeH$_3^{\bullet}$ model successfully reproduces what our CASSCF and CASPT2 calculations predict to occur in planar O(SiH$_2$)$_3^{\bullet+}$: the quartet becomes the ground state.

In understanding why the quartet falls below the doublet in both O(SiH$_2$)$_3^{\bullet+}$ and in our HeH$_3^{\bullet}$ model for it, eq 14 is useful. It gives the wave function for the $^2E_x'$ component of $^2E'$ in HeH$_3^{\bullet}$. Equation 14 differs from eq 13 by the fact that each configuration in eq 14 contains a term, He^2, for the two electrons that occupy the 1s AO on helium. However, as in eq 13, ψ_1, ψ_2, and ψ_3 are the combinations of hydrogen defined by eqs 4−6.

$$^2\Psi_x = c_1|\text{He}^2\psi_1{}^2\psi_2{}^\alpha\rangle - c_2|\text{He}^2\psi_2{}^\alpha\psi_3{}^2\rangle - \frac{c_3}{\sqrt{2}}(|\text{He}^2\psi_1{}^\alpha\psi_2{}^\alpha\psi_3{}^\beta\rangle - |\text{He}^2\psi_1{}^\alpha\psi_2{}^\beta\psi_3{}^\alpha\rangle) \quad (14)$$

In HeH$_3^{\bullet}$, ψ_2 and ψ_3 each have a node at the He atom, but ψ_1 has the correct symmetry to interact with the He 1s AO. Since ψ_1 interacts with this doubly occupied orbital of much lower energy, ψ_1 is destabilized by this interaction.

Table 4 shows how the coefficients of the configurations in the $^2E'$ wave functions change as the He−H distance, R, decreases and the interaction between ψ_1 and the He 1s AO increases. Since ψ_1 is destabilized by its interaction with the He 1s AO, at values of R < 2.5 Å the coefficient, c_2, of the configuration in which ψ_1 is empty increases at the expense of c_1, the coefficient of the configuration in which ψ_1 is doubly occupied. As R decreases, c_3, the coefficient of the configurations in which ψ_1 is singly occupied also decreases, but to a much lesser extent than does c_1.

Nevertheless, at He−H distances, where the increases in the energies of both $^2E'$ and $^4A_2'$ show that there is a nonnegligible interaction between the 1s orbitals of these atoms (e.g., at R = 2.0 Å), the coefficients c_1, c_2, and c_3 remain nearly equal. The reason is that, as the He−H distance decreases, the H−H distances also decrease. Although the He−H interactions in ψ_1 are antibonding in HeH$_3^{\bullet}$, the H−H interactions in ψ_1 are bonding in HeH$_3^{\bullet}$, as they are in H$_3^{\bullet}$. These two opposing effects on the energy of ψ_1 are what tend to keep the coefficients c_1, c_2, and c_3 nearly equal, until values of R are reached at which He−H antibonding dominates H−H bonding (e.g., at R = 1.0 Å).

As already discussed, when these coefficients are equal or nearly so, the quartet has the advantage of having a slightly lower Coulombic repulsion energy than the doublet, because the Pauli principle prevents electrons of the same spin from simultaneously appearing in the overlap regions between atoms. Thus, at geometries of HeH$_3^{\bullet}$ where an appreciable fraction of the He−H antibonding interactions in the doublet are canceled by H−H bonding interactions, the lower Coulombic repulsion in the quartet can become the dominant energetic effect and cause $^4A_2'$ to fall below $^2E'$.

Comparison of the CASSCF coefficients for the configurations in the $^2E'$ wave functions in Tables 3 and 4 shows that, at the same values of R (e.g., R = 1.5 Å), c_1 and c_2 are more nearly equal in HeH$_3^{\bullet}$ than in H$_3^{\bullet}$. Similarly, one would expect the CASSCF coefficients for the configurations in the $^2A_2$ wave functions that correspond to the first two configurations in eqs 13 and 14 to be more nearly equal in O(SiH$_2$)$_3^{\bullet+}$ than in AlO$_3^{\bullet}$. In fact, at the equilibrium geometries of the doublet states of these two radicals, $(c_2/c_1)^2$ = 1.12 in O(SiH$_2$)$_3^{\bullet+}$, but $(c_1/c_2)^2$ = 1.23 in AlO$_3^{\bullet}$. [29]

Conclusions

Our CASSCF, CASPT2, and UB3LYP calculations all predict AlO$_3^{\bullet}$ to have a doublet ground state; whereas, the same types of calculations all predict the ground state of O(SiH$_2$)$_3^{\bullet+}$ to be

Heteroatom Analogues of TMM Radical Ions

J. Phys. Chem. A, Vol. 106, No. 12, 2002 **2969**

a quartet. Model calculations on $H_3^•$ and $HeH_3^•$ support the following explanation for this difference between $AlO_3^•$ and $O(SiH_2)_3^{•+}$.

In $AlO_3^•$ the Al−O and the O−O π interactions both selectively stabilize the $1a_2''$ bonding MO and, hence, favor the doublet state over the quartet. In contrast, in $O(SiH_2)_3^{•+}$ destabilization by O−Si π antibonding of the $2a_2''$ MO that is largely localized on the silicons is partially offset by Si−Si π bonding. As a result, occupancy of this π MO is not strongly disfavored, relative to occupancy of an e' nonbonding MO. Consequently, in $O(SiH_2)_3^{•+}$ the lower electron repulsion in the quartet can overcome the only slightly larger amount of π bonding in the doublet.

More generally, the results described in this paper predict that the ground state of an XY_3 radical with three π electrons will always be a doublet, even if Y is much more electronegative than X. In contrast, in an XY_3 radical with five π electrons, if X is much more electronegative than Y, there is at least a possibility that the ground state will be a quartet.

We hope that our predictions of how ΔE_{DQ} depends on the electronegativities of X and Y in XY_3 radicals with three and with five π electrons will be useful in designing XY_3 radicals with very low-lying excited quartet states. We also hope our predictions—that the doublet will be the ground state of every XY_3 radical with three π electrons, but that the quartet can become the ground state of a planar XY_3 radical with five π electrons, when X is much more electronegative than Y—will stimulate experimental tests.

Supporting Information Available: Optimized geometries and energies of all the radicals in Tables 1 and 2. This material is available free of charge via the Internet at http://pubs.acs.org.

References and Notes

(1) See: Coulson, C. A. *J. Chim. Phys.* **1948**, *45*, 243.

(2) Dowd, P. *J. Am. Chem. Soc.* **1966**, *88*, 2587.

(3) For reviews, see, for example: (a) Dowd, P. *Acc. Chem. Res.* **1972**, *5*, 242. (b) Berson, J. A. *Acc. Chem. Res.* **1978**, *11*, 446. (c) Borden, W. T.; Davidson, E. R. *Acc. Chem. Res.* **1981**, *14*, 69. (d) Berson, J. A. In *Diradicals*; Borden, W. T., Ed.; J. Wiley and Sons: New York, 1982; Chapter 4.

(4) (a) Dowd, P.; Sachdev, K. *J. Am. Chem. Soc.* **1967**, *89*, 715. (b) Dowd, P.; Gold, A.; Sachdev, K. *J. Am. Chem. Soc.* **1968**, *90*, 2715. (c) Basemen, R. J.; Pratt, D. W.; Chow, M.; Dowd, P. *J. Am. Chem. Soc.* **1976**, *98*, 5726.

(5) See, for example: (a) Davidson, E. R.; Borden, W. T.; *J. Am. Chem. Soc.* **1977**, *99*, 2053. (b) Borden, W. T. In *Diradicals*; Borden, W. T., Ed.; J. Wiley and Sons: New York, 1982; pp 1−72.

(6) Ovchinnikov, A. A. *Theor. Chim. Acta* **1978**, *47*, 297.

(7) (a) Wenthold, P. G.; Hu, J.; Squires, R. R.; Lineberger, W. C. *J. Am. Chem. Soc.* **1996**, *118*, 475. (b) Wenthold, P. G.; Hu., J.; Squires, R. R.; Lineberger, W. C. *J. Am. Soc. Mass Spectrom.* **1999**, *10*, 800−809.

(8) (a) Cramer, C. J.; Smith, B. A. *J. Phys. Chem.* **1996**, *100*, 9664. (b) For a recent review of singlet−triplet splittings in non-Kekule hydrocarbon diradicals, see: Borden, W. T. In *Magnetic Properties of Organic Materials*; Lahti, P., Ed..; Marcel Dekker: New York, 1999; pp 61−102.

(9) Komaguchi, K.; Shiotani, M.; Lund, A. *Chem. Phys. Lett.* **1997**, *265*, 217.

(10) Du, P.; Borden, W. T. *J. Am. Chem. Soc.* **1987**, *109*, 5330.

(11) (a) Takahashi, Y.; Miyashi, T.; Mukai, T. *J. Am. Chem. Soc.* **1983**, *105*, 6511. (b) Miyashi, T.; Takahashi, Y.; Mukai, T.; Roth, H. D.; Schilling, M. L. M. *J. Am. Chem. Soc.* **1985**, *107*, 1079. (c) Miyashi, T.; Kamata, M.; Mukai, T. *J. Am. Chem. Soc.* **1986**, *108*, 2755.

(12) Itoh, T.; Matsuda, K.; Iwamura, H.; Hori, K. *J. Am. Chem. Soc.* **2000**, *122*, 2567.

(13) (a) Harihan, P. C.; Pople, J. A. *Theor. Chim. Acta* **1973**, *28*, 213. (b) Clark, T.; Chandrasekhar, J.; Spitznagel, G. W.; Schleyer, P. v. R. *J. Comput. Chem.* **1983**, *4*, 294.

(14) Becke, A. D. *J. Chem. Phys.* **1993**, *98*, 5648.

(15) Lee, C.; Yang, W.; Parr, R. G. *Phys. Rev. B* **1988**, *37*, 785.

(16) Frisch, M. J.; Trucks, G. W.; Schlegel, H. B.; Scuseria, G. E.; Robb, M. A.; Cheeseman, J. R.; Zakrzewski, V. G.; Montgomery, J. A., Jr.; Stratmann, R. E.; Burant, J. C.; Dapprich, S.; Millam, J. M.; Daniels, A. D.; Kudin, K. N.; Strain, M. C.; Farkas, O.; Tomasi, J.; Barone, V.; Cossi, M.; Cammi, R.; Mennucci, B.; Pomelli, C.; Adamo, C.; Clifford, S.; Ochterski, J.; Petersson, G. A.; Ayala, P. Y.; Cui, Q.; Morokuma, K.; Malick, D. K.; Rabuck, A. D.; Raghavachari, K.; Foresman, J. B.; Cioslowski, J.; Ortiz, J. V.; Stefanov, B. B.; Liu, G.; Liashenko, A.; Piskorz, P.; Komaromi, I.; Gomperts, R.; Martin, R. L.; Fox, D. J.; Keith, T.; Al-Laham, M. A.; Peng, C. Y.; Nanayakkara, A.; Gonzalez, C.; Challacombe, M.; Gill, P. M. W.; Johnson, B. G.; Chen, W.; Wong, M. W.; Andres, J. L.; Head-Gordon, M.; Replogle, E. S.; Pople, J. A. *Gaussian 98*, revision A.7; Gaussian, Inc.: Pittsburgh, PA, 1998.

(17) (a) Schmidt, M. W.; Baldridge, K. K.; Boatz, J. A.; Elbert, S. T.; Gordon, M. S.; Jensen, J. H.; Koseki, S.; Matsunaga, N.; Nguyen, K. A.; Su, S. J.; Windus, T. L.; Dupuis, M.; Montgomery, J. A. *J. Comput. Chem.* **1993**, *14*, 1347. (b) Bode, B. M.; Gordon, M. S. *J. Mol. Graphics Modell.* **1999**, *16*, 133.

(18) Borden, W. T.; Davidson, E. R. *Acc. Chem. Res.* **1996**, *29*, 67.

(19) (a) Andersson, K.; Malmqvist, P.-Å.; Roos, B. O.; Sadlej, A. J.; Wolinski, K. *J. Phys. Chem.* **1990**, *94*, 5483. (b) Andersson, K.; Malmqvist, P.-Å.; Roos, B. O. *J. Chem. Phys.* **1992**, *96*, 1218.

(20) Andersson, K.; Blomberg, M. R. A.; Fülscher, M. P.; Karlström, G.; Lindh, R.; Malmqvist, P.-Å.; Neogrády, P.; Olsen, J.; Roos, B. O.; Sadlej, A. J.; Schütz, M.; Seijo, L.; Serrano-Andrés, L.; Siegbahn, P. E. M.; Widmark, P.-O. *MOLCAS*, version 4.1; Department of Theoretical Chemistry, Chemical Centre: University of Lund, P.O. Box 124, S-221 00 Lund, Sweden, 1997.

(21) For detailed discussions of artifactual symmetry breaking in similar molecules, see: Davidson, E. R.; Borden, W. T. *J. Phys. Chem.* **1983**, *87*, 4783.

(22) Jahn, H. A.; Teller, E. *Proc. R. Soc. London, Ser. A* **1937**, *116*, 605.

(23) See, for example: (a) Schmidt, M. W.; Truong, P. N.; Gordon, M. S. **1987**, *109*, 5217. (b) Wiberg, K. B.; Nakaji, D. *J. Am. Chem. Soc.* **1993**, *115*, 10658.

(24) This $H_3^•$ model breaks down if distortions from D_{3h} geometries are allowed; since the Jahn−Teller-active vibrational modes in $^2E'$ lead to stationary points with highly distorted geometries. One stationary point corresponds to a hydrogen molecule plus a distant hydrogen atom at a C_{2v} geometry, and another stationary point corresponds to a linear geometry, with equal H−H bond lengths, that is the transition structure for the $H_2 + H^•$ reaction.

(25) It is easy to use eqs 2 and 3 to show that electrons of opposite spin can appear simultaneously in the overlap regions between ϕ_1 and ϕ_2 and between ϕ_1 and ϕ_3 in $^2\Psi_x$ and between ϕ_2 and ϕ_3 in $^2\Psi_y$.

(26) If overlap were included in normalizing the MOs in eqs 4−6, in eqs 7−9 the coefficients of ψ_1 would increase, and those of ψ_2 and ψ_3 would decrease. Therefore, with inclusion of overlap in the normalization, the weight of the first configuration in eqs 11 and 12 would be larger than the weight of the second configuration; and the combined weights of the last two configurations would have an intermediate value. Consequently, when overlap is significant, constraining the weights of the configurations in eqs 11 and 12 to be equal disadvantages these doublet wave functions, relative to the quartet, by making the doublets overall slightly antibonding, rather than nonbonding.

(27) Squires, et al. have measured EA = 9.9 kcal/mol for $C(CH_2)_3^{•−}$,[7] in fair agreement with the value of EA = 5.3 kcal/mol, computed by UB3LYP. The agreement between the calculated and experimental EAs is further improved if the CH_2 groups in $C(CH_2)_3^{•−}$ are allowed to pyramidalize, which lowers the energy of the radical anion by 0.4 kcal/mol, and gives EA = 5.7 kcal/mol.

(28) Unconstrained reoptimization of the geometry of the quartet led to a C_1 structure, with all the silyl centers pyramidalized, which was 46.4 kcal/mol lower in energy than planar $^4A_2''$. Attempts to reoptimize the geometry of the lowest planar doublet led, unfortunately, to pyramidalization accompanied by Si−Si bond formation. However, constrained optimization of a $^2A''$ wave function, with a plane of symmetry perpendicular to the molecular plane, led to a C_s geometry with the two equivalent silyls pyramidalized in the opposite direction than the third. The energy of this doublet was computed to be 0.2 kcal/mol lower than that of the fully optimized quartet.

(29) In $O(SiH_2)^{•+}$, the two unique bond lengths at the CASSCF-optimized C_{2v} geometry of the $^2A_2$ state ($R = 1.788$ and 1.789 Å) are computed to be only slightly longer than those in the same state of $AlO_3^•$ ($R = 1.741$ Å and 1.742 Å). When the CASSCF calculation on $O(SiH_2)^{•+}$ was repeated at the CASSCF-optimized geometry of $AlO_3^•$, the ratio $(c_2/c_1)^2$ at the equilibrium geometry of $O(SiH_2)^{•+}$ was essentially unchanged.